

THE PHYSICAL REVIEW

A journal of experimental and theoretical physics established by E. L. Nichols in 1893

SECOND SERIES, VOL. 84, No. 3

NOVEMBER 1, 1951

Photoneutron Thresholds*†

R. SHER, J. HALPERN, AND A. K. MANN
University of Pennsylvania, Philadelphia, Pennsylvania
(Received July 12, 1951)

A 25-Mev betatron is used to measure the photoneutron thresholds of 77 isotopes by direct detection of neutron yields as a function of maximum bremsstrahlung energy. The neutrons, moderated in paraffin, are observed with a BF_3 proportional counter and time delay circuits. Threshold energies for 31 isotopes are repetitions of previously reported values from other laboratories and those for 46 isotopes are either new or more precise determinations.

INTRODUCTION

MEASUREMENT of neutron binding energies is one method of establishing mass differences with great accuracy. In conjunction with other data, this permits mass assignments to intermediate and heavy nuclei. Such measurements also provide information about current models of nuclear structure.

The reactions from which neutron binding energies can be obtained are: (1) (p,d) , (d,t) , and (γ,n) , in which a neutron is removed from a target nucleus; and (2) (d,p) and (n,γ) , in which a neutron is added. In general, those reactions in which the incident particles are charged yield either upper or lower limits to the neutron binding energies, because it is difficult to be sure that direct transitions to the ground state of the product nucleus are involved. The reactions (1) furnish neutron binding data on the target isotope, while reactions (2) give similar data for the residual nucleus. Harvey¹ has summarized the experimental data for some 80 isotopes. Of these, 38 have been investigated by the measurement of (γ,n) threshold energies in which betatrons were used as sources of excitation.² Yields of the (γ,n) reactions

are measured as a function of maximum bremsstrahlung energy and the threshold determined by some suitable extrapolation to zero yield. In most cases, the yield of the reaction was obtained by measurement of the radioactivity of the product nucleus. In a few cases, rhodium and iodine detectors were used to observe the neutrons from the reaction. The primary advantage of detecting neutrons rather than residual radioactivity is the possibility of measuring (γ,n) processes whose products are either stable or have very long or very short half-lives. On the other hand, a disadvantage is that identification of isotopes becomes more difficult when elements of natural isotopic composition are bombarded.

This paper will report on the measurement of (γ,n) threshold energies of 77 isotopes by a new method³ in which neutrons are directly detected in a boron-trifluoride proportional counter. This method preserves the advantages of direct neutron detection and also permits rapid measurements which are independent of the conditions of bombardment.

DESCRIPTION OF APPARATUS

An enriched BF_3 proportional counter was imbedded in the center of a paraffin block $9'' \times 9'' \times 20''$, as shown in Fig. 1. The collimated bremsstrahlung beam from the betatron, which was $\frac{1}{2}$ inch in diameter at the collimator exit, passed through a $\frac{3}{4}$ -inch-diameter hole running the length of the block and containing at its center the sample to be irradiated. Without a sample in position, the beam passed through the block undisturbed. Shielding against background neutrons was

* Part of a dissertation submitted by R. Sher in fulfillment of the requirements for the Ph.D. degree from the Graduate School of the University of Pennsylvania.

† Supported in part by the joint program of the AEC and ONR.

¹ J. A. Harvey, *Phys. Rev.* **81**, 353 (1951).

² a. G. C. Baldwin and H. W. Koch, *Phys. Rev.* **67**, 1 (1945); b. McElhinney, Hanson, Becker, Duffield, and Diven, *Phys. Rev.* **75**, 542 (1949); c. Hanson, Duffield, Knight, Diven, and Palevsky, *Phys. Rev.* **76**, 578 (1949); d. H. Palevsky and A. O. Hanson, *Phys. Rev.* **79**, 242 (1950); e. W. E. Ogle and R. E. England, *Phys. Rev.* **78**, 63 (1950); f. Ogle, Brown and Carson, *Phys. Rev.* **78**, 63 (1950); g. R. W. Parsons and C. H. Collie, *Proc. Phys. Soc. (London)*, **A63**, 839 (1950); h. Parsons, Lees, and Collie, *Proc. Phys. Soc. (London)*, **A63**, 915 (1950).

³ Sher, Halpern, and Stephens, *Phys. Rev.* **81**, 154 (1951).

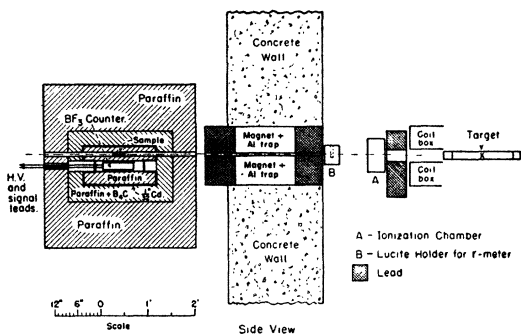


FIG. 1. Arrangement of apparatus.

obtained by surrounding the apparatus with a $\frac{1}{32}$ inch cadmium sheet, then with 4 inches of paraffin mixed with B_4C (30 percent by weight of B_4C), and finally with 12 inches of additional paraffin. Samples, from 5 to 50 grams of high purity material of natural isotopic abundance, and in powder or lump form, were placed in $\frac{3}{4}$ inch diameter thin-walled aluminum cylinders and irradiated axially. The axis of the counter (2 in. diameter, 12 in. active length, filled to a pressure of 40 cm with BF_3 enriched to 96 percent B^{10}) was parallel to and one inch from the center of the x-ray beam. The distance from the sample to the betatron target was 8.5 feet.

The x-ray beam consists of a series of sharp pulses, $0.5\mu\text{sec}$ in half-width, which on striking the sample produce a neutron intensity of similar time duration. This is repeated every $5550\mu\text{sec}$. The BF_3 counter, which essentially detects only slow neutrons falling within its sensitive volume, will then record neutrons from the sample during a time interval dependent on the velocity distribution of neutrons leaving the sample and on the geometry of the apparatus and its effect on the diffusion time. Counts from neutrons produced outside the paraffin housing arise mainly from (γ, n) reactions in the betatron target and in the lead collimator. Those that leak through to the counter have a time distribution principally determined by the geometry of the betatron room because, in general, they have suffered collisions in the concrete shielding shown in Fig. 1 and in the walls of the room.

During the $0.5\mu\text{sec}$ time that the x-ray beam is on, the counter experiences a large pile-up of secondary electrons. The effect of pile-up was eliminated by means of a gated counting circuit, the parameters of which were determined from a study of the time distributions mentioned above. The counting circuit is represented schematically in Fig. 2. Pulses from the counter, which was operated at 2600 volts, are amplified in Atomic Instrument Company Mod. 205 and Mod. 204B pre-amplifier and amplifier, and after pulse-height discrimination are fed to one channel of a coincidence circuit of conventional design. The other channel of the coincidence circuit receives a gate which is triggered by the same pulse that fires the betatron expander circuit.

This gate is of variable delay and time duration. The output of the coincidence circuit enters a scaler which records counts from the counter only during the gate duration.

A lower limit to the delay time of the gate was required by amplifier overloading which resulted from the pile-up. For maximum betatron intensity and a high Z sample, the amplifier fully recovered in about $15\mu\text{sec}$. It was necessary for the gate to be of sufficient duration to allow most of the delayed neutrons to be counted. The diffusion time of the neutrons in our geometry was measured by varying the position of the gate in the interval between betatron pulses. It was found that neutrons from a sample arrived at the counter with an exponentially decreasing time distribution of half-width $100\mu\text{sec}$. Similar measurements of the background neutrons gave a value of about $600\mu\text{sec}$, for the half-width. For all further measurements, the time delay and duration of the gate were fixed at 30 and $300\mu\text{sec}$, respectively.

The maximum bremsstrahlung energy was varied by expanding the electron beam of the betatron at a given value of the magnetic field using circuits similar to those previously developed.⁴ The desired value of the magnetic field was measured by the voltage across a condenser in series with a large resistance both of which were across one of the magnet coils. This is indicated as "integrator stack" in the block diagram of Fig. 3. The voltage across the condenser at any time is proportional to the voltage applied to the magnet coil and hence to the magnetic field at the electron orbit. The condenser voltage was used to fire a trigger circuit whose bias was

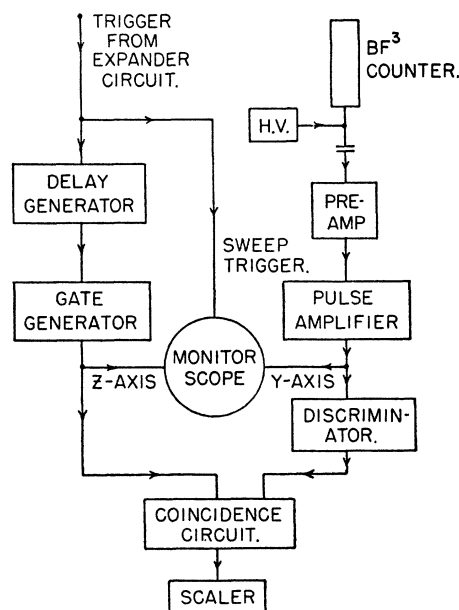


FIG. 2. Block diagram of counting circuits.

⁴ McElhinney, Hanson, Becker, Duffield, and Diven, *Phys. Rev.* **75**, 542 (1949); Katz, McNamara, Forsyth, Haslam, and Johns, *Can. J. Research* **A28**, 113 (1950).

fixed by the setting of the energy control potentiometer, hereafter called helipot. The trigger so generated, activated both the expander coils and the counter gate as mentioned above. The helipot reading was then a direct measure of the maximum x-ray energy.

PROCEDURE

In the measurement of thresholds, the neutron yields per roentgen of radiation corresponding to various maximum energies of the x-ray beam (helipot settings) were measured. The total number of roentgens striking the sample at a given helipot setting was determined with a 250 r Victoreen thimble meter imbedded in a Lucite cylinder of 8 cm diameter and located 3 feet from the betatron target. The cylinder and r-meter remained in the beam throughout the experiment. The absolute measurement of r was not required. For low Z elements, where the neutron yields are small, the samples were irradiated with about 100 r at each energy point, while for the high Z elements 50 r was sufficient. A complete run on a sample required about four hours. Two independent and complete sets of data, separated in time by at least several days, were obtained for most of the samples. At the beginning and end of each day, the yield curves for two elements selected as standards were measured. This served both as an over-all performance check of the apparatus and to determine the stability of the energy scale. Manganese and bismuth were chosen as standards because of their single isotopic con-

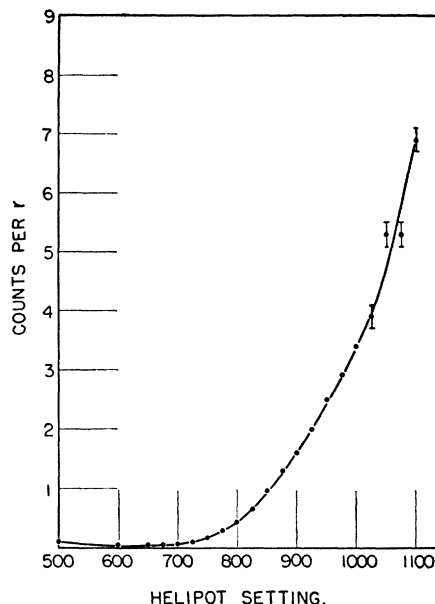


FIG. 4. Background dependence on energy.

stitutions, adequate neutron yields, and convenient thresholds.

The counting rate occurring without a sample in the target position, but with the aluminum sample holder in place, was measured over the entire energy range covered in the experiment, and with about 1000 r total irradiation at each energy point. Background measurements at various times in the course of the experiment were in agreement within statistical errors.

In order to obtain threshold values it is necessary to extrapolate the yield data from a given sample to zero yield. If the shape of the yield curve around threshold were known, it would be possible to make an unambiguous extrapolation providing no distortions of this shape were produced by counting losses and x-ray absorption in the sample. The effect of counting losses was found experimentally by observing the counting rate from a sample bombarded with bremsstrahlung of fixed high maximum energy but varying intensity. This counting loss curve was in agreement with the curve calculated on the basis of the neutron time distribution. The counting loss corrections to the yield data were seldom greater than two percent and never greater than five percent. Data taken with lead samples of several thicknesses indicated that x-ray absorption did not affect the shapes of the yield curves.

The relationship between the yield and energy is determined by the energy dependence of the cross section of the reaction, the bremsstrahlung and the detection efficiency of the apparatus. These factors are too complex for individual determination. We find, as do Parsons and Collie,²⁸ that all of our data can be represented by the relation $Y \sim (E - E_0)^m$, where Y is the yield, E is the maximum x-ray energy, m is a constant for a given isotope, and E_0 is taken to be the

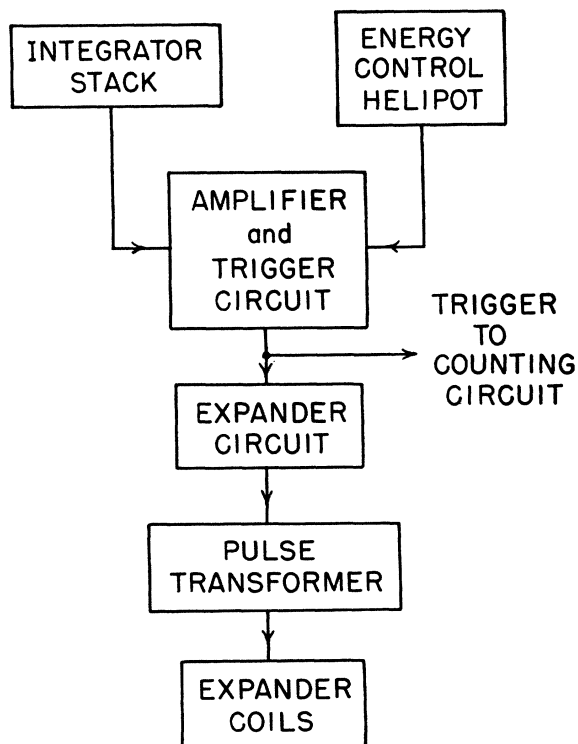


FIG. 3. Block diagram of energy control circuits.

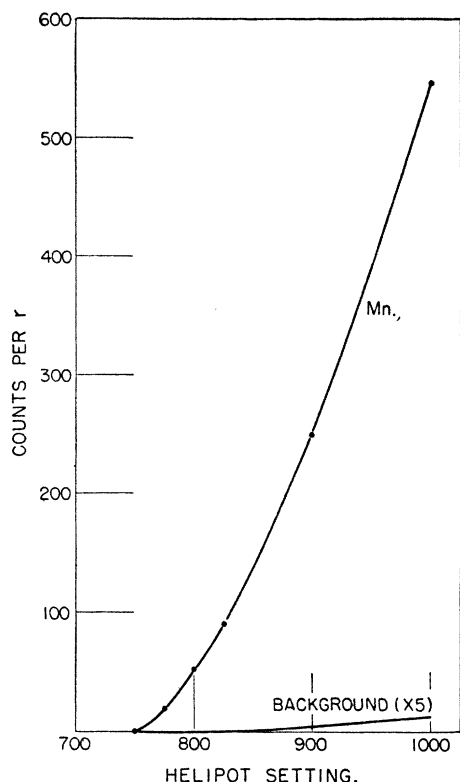


FIG. 5. Yield curve for manganese. The background is shown expanded five times.

threshold energy. In practice, E_0 and m are determined graphically by trial. It is probable that other representations would be equally satisfactory. The justification

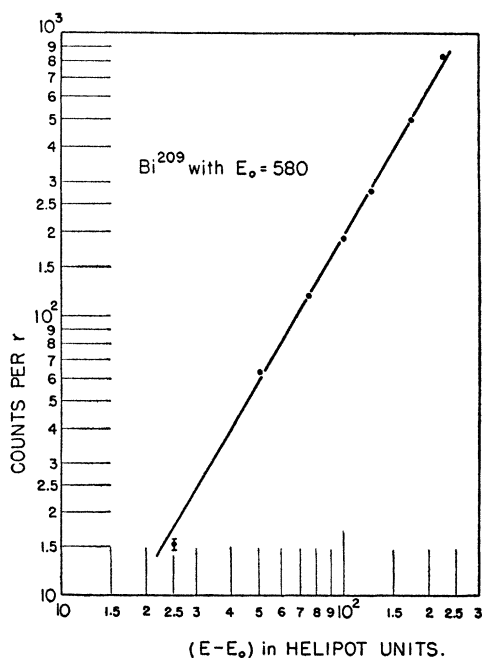


FIG. 6. Illustration of the graphical method of obtaining a threshold energy from the yield data for bismuth.

of the method used here lies in its convenience in treating the data and in the agreement of the results with known thresholds.

RESULTS

A curve showing the background as a function of helipot setting is presented in Fig. 4. Below 600, the background is primarily due to cosmic rays and Ra-Be sources in the laboratory. This is evidenced by the fact that the background is independent of the betatron beam in this helipot region. Consequently, while the background counts per minute are independent of the helipot setting in this region, the counts per r will rise with decreasing helipot setting because of the decreasing r per minute output of the betatron. Above 600, the background rises sharply because of the onset of (γ, n) reactions in the platinum betatron target and lead collimator. Figure 5 shows the yield curve for manganese, which has a moderate neutron yield, and the background curve magnified fivefold.

The graphical method of obtaining a threshold energy from the yield data are illustrated in the log-log plot of Fig. 6. The data are for bismuth, a singly isotopic element, for which the threshold value is known to be 7.44 Mev.⁵ For an $E_0 = 580$ helipot units, corresponding to the known threshold energy, the data form a straight line over an energy interval of about 3.5 Mev, which is the entire region covered. If a value of E_0 differing from 580 by ± 10 units (approximately 0.15 Mev) is chosen the plot deviates strongly from a straight line.

Figure 7 shows a similar plot for iron, a multiply isotopic element. The abrupt change in slope of curve *A* is due to the contribution to the yield of a second isotope with higher threshold. The straight line of lesser slope was obtained using a value of $E_0 = 600$ helipot units, corresponding to the known threshold of Fe^{57} at 7.65 Mev.¹ It should be noted that the relative abundance of Fe^{57} is 2.1 percent. If the yield from Fe^{57} is extrapolated to higher energies and subtracted from the total yield, the data for the isotope with higher threshold may be plotted in the same manner as before. This plot, for which $E_0 = 810$ helipot units, is shown as curve *B*, and can be assigned to Fe^{56} . Of the remaining isotopes, Fe^{54} is known to have a threshold of 13.8 Mev,^{2b} which is not observable in our experiment because of the small relative abundance of Fe^{54} (6.0 percent) compared to that of Fe^{56} (91.6 percent). The abundance of Fe^{58} (0.3 percent) is also too small to permit its observation. The threshold energy of 11.15 Mev corresponding to the helipot reading for Fe^{56} is in agreement with the lower limit of 11.3 Mev predicted by Harvey.¹

Another example of the data for a multiply isotopic element, bromine, is shown in Fig. 8. The presence of both Br^{79} (50.6 percent) and Br^{81} (49.4 percent) is clearly indicated. The straight line for Br^{81} is obtained for a threshold energy of 9.95 Mev, and that for Br^{79}

⁵ J. A. Harvey, Phys. Rev. 79, 241 (1950).

is for 10.60 Mev. These values are in agreement with those obtained by McElhinney *et al.*^{2b} who find 10.2 and 10.7 Mev respectively, using the radioactivity method of observing (γ, n) reactions. Our bromine data were obtained from a sample of NaBr. The threshold for Na²³ (100 percent) occurs at about 12.0 Mev, and consequently the yield from sodium does not interfere with the bromine measurements.

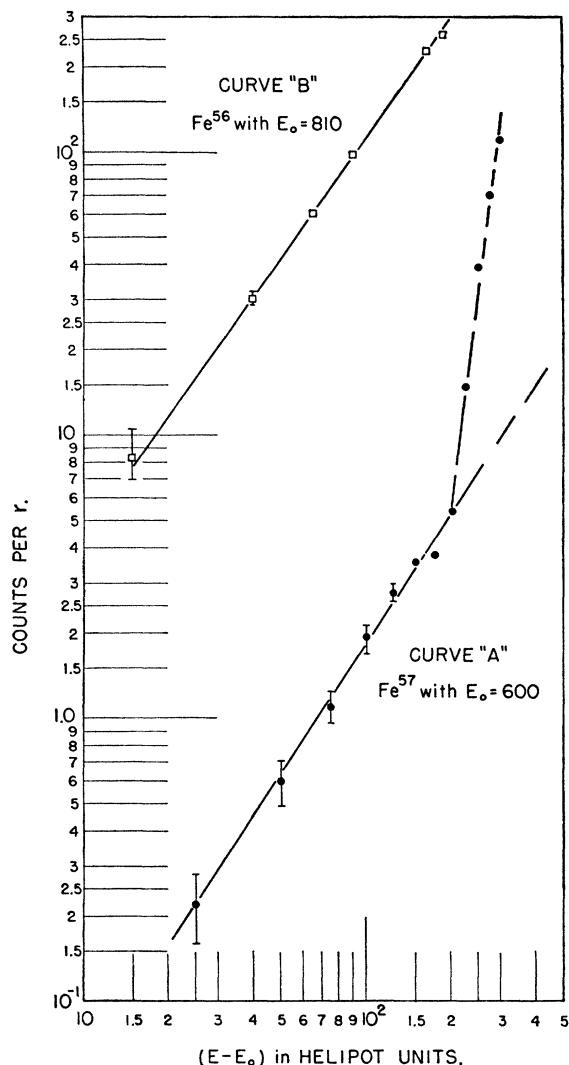


FIG. 7. Illustration of the graphical method for two isotopes of iron.

As a final illustration, the data for zinc, which are somewhat unusual, are presented in Fig. 9. Because of a fortuitous arrangement of yields, abundances, and thresholds, four of the five stable isotopes are clearly delineated; Zn⁷⁰ with an abundance of 0.5 percent and a threshold energy of 9.2 Mev^{2c} cannot be seen. The first threshold, which occurs at 6.95 Mev in Fig. 9, is assigned to Zn⁶⁷, which according to the mass formula should have a threshold at least 2 Mev below the threshold for any other isotope. Furthermore, the

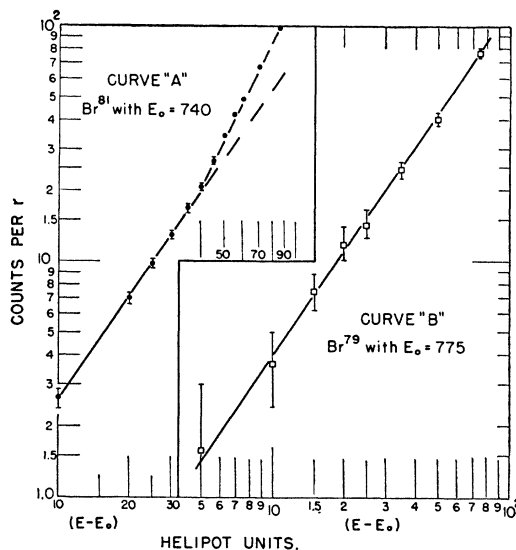


FIG. 8. Data for bromine showing the resolution of the two isotopes.

relative abundance of Zn⁶⁷ (3.9 percent) is small compared to that of the other four isotopes and unless it had the lowest threshold it would not be detected. The assignments of 10.15 Mev to Zn⁶⁸ and of 11.15 Mev to Zn⁶⁶ are also based on the mass formula and relative abundance data, but are subject to more uncertainty. We find the threshold for Zn⁶⁴ at 11.6 Mev which is in agreement with the value obtained by Hanson *et al.*^{2c} (11.8 Mev) using the radioactivity method.

The procedure illustrated above has been applied to the data for 77 isotopes of 48 elements. The threshold

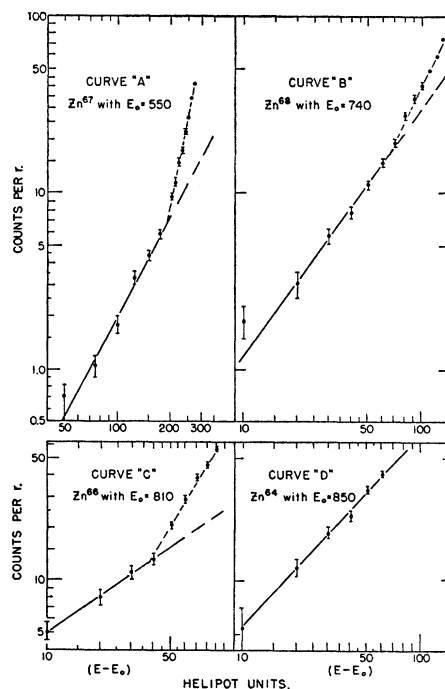


FIG. 9. Data for zinc showing resolution of four isotopes.

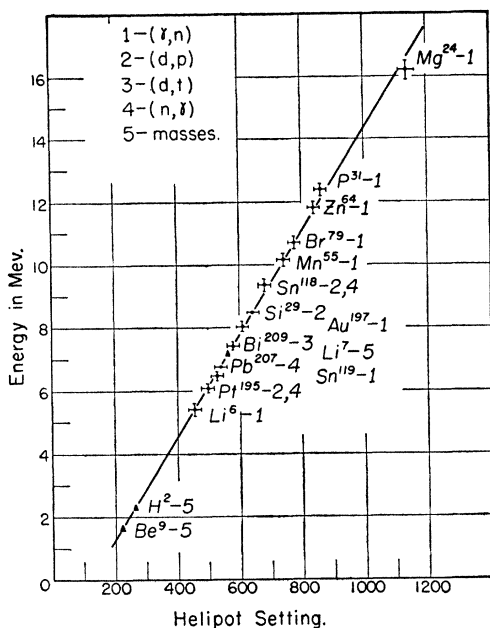


FIG. 10. Betatron energy scale.

energies of 40 isotopes represent new determinations and those of 6 isotopes are improvements in previous precision.

There are two primary factors which limit the precision of the measured thresholds, namely, the energy scale and the statistical uncertainties of the data. To calibrate the energy scale, we have obtained helipot settings corresponding to the thresholds of beryllium, deuterium and Li^7 , for which the energies at threshold are well known. These cover the energy interval from 1.67 to 7.15 Mev and should serve as a calibration provided the relation between helipot and energy is linear within the statistical errors of the measurements. This linearity is well substantiated by the agreement in absolute value of threshold energies obtained in other laboratories with our energy scale, which is shown in Fig. 10.

Since the measurements of thresholds extended over a period of three months, it was necessary to determine the stability of the energy scale. Daily threshold measurements on the two standards, Mn and Bi, taken during the entire course of the experiment, exhibited a maximum spread of 0.15 Mev. We therefore assign a mean deviation of 0.10 Mev to the absolute threshold energies due to fluctuations in the energy scale.

In general, the statistical errors contributed an uncertainty in the value of a threshold determination which was about half that due to the energy scale fluctuations. In some isotopes, a combination of low isotopic abundance, low yield and high threshold (relatively high background), increased the statistical error. In no case did the total error exceed ± 0.30 Mev.

In the interpretation of the data for those elements with many isotopes of approximately equal abundances

it was sometimes not possible to be certain that two or more isotopes did not contribute to the measured yield curve from which a single threshold was obtained. The threshold values for elements in which this lack of resolution might have influenced the measurements are appropriately indicated in the summary of results. We have also indicated the degree of certainty of isotopic assignment by classifying the assignments as certain (class A), probable (class B), and doubtful or unknown (class C).

Table I summarizes the results of the experiment. The preliminary values for 31 threshold energies contained in a previous publication,³ are in agreement with the data in Table I with the exception of B^{10} and Sr^{87} . The original data for B^{10} were influenced by low yield and sample impurity, and upon repetition using a pure sample the thresholds of both B^{10} and B^{11} agreed within experimental error with the values computed from known masses. The error in the previous value given for Sr^{87} was the result of our inability to resolve Sr^{86} and Sr^{87} . It should be noted that the value for Sr^{87} given in Table I is in agreement with the results of (n, γ) and (d, p) measurements.

The value for Li^6 is to be compared with the result given by Titterton and Brinkley,⁶ who made photographic emulsion measurements of the ranges of the alpha-particle and proton resulting from the decay of Li^6 produced in the reaction $\text{Li}^6 + h\nu \rightarrow \text{Li}^5 + n$. If we assume that the neutrons detected in our apparatus are from the above reaction, the ground-state energy of Li^5 so determined is in excellent agreement with their results. However, the reaction $\text{Li}^6 + h\nu \rightarrow \text{He}^5 + p$ should have a threshold some 0.8 Mev lower, and the subsequent break-up of He^5 should contribute to the neutron yield. Similarly, the photographic emulsion work would show a group of long-range protons resulting from the second mode of disintegration of Li^6 . The absence of the latter reaction in our threshold measurements could be due to inability to resolve these thresholds if the $\text{He}^5 + p$ yield is suppressed sufficiently by the coulomb barrier. The reaction $\text{Li}^6 + h\nu \rightarrow \alpha + p + n$, with still lower threshold, is probably suppressed by selection rules.

Our threshold measurements show three discrepancies with previously quoted values. The threshold value for Al^{27} of 12.75 Mev is in better agreement with that of 11.1 ± 2 computed from masses than the (γ, n) threshold of 14.0 ± 0.4 previously quoted.^{2b} The 14-Mev value was obtained from observation of the 7 sec radioactivity in Al^{26} .

Although we find a value for Cu^{63} in good agreement with values obtained from radioactivity measurements, our value for Cu^{65} is outside the combined errors of the two measurements.^{2b}

Harvey¹ computed a lower limit to the threshold of La^{139} from the $\text{Ba}^{138}(d, p)$ reaction and the disintegration schemes of Ba^{139} and La^{138} . The value he used for the

⁶ E. W. Titterton and T. A. Brinkley, Proc. Phys. Soc. (London) 64A, 212 (1951).

TABLE I. Summary of results.

Isotope	Percent abundance	Present measurements				Previous measurements		Reference	Threshold from mass formulat
		Threshold (Mev)	Error (Mev)	<i>m</i>	Class	Threshold (Mev)	Method		
H ²		2.23	Calib.	1.8	A	2.23	masses		
Li ⁶	7.5	5.35	0.20	1.0	A	5.4±0.2	(γ, n)	‡	4.38
Li ⁷	92.5	7.15	Calib.	1.0	A	7.15±0.07	masses		15.47
Be ⁹	100	1.67	Calib.	0.9	A	1.67±0.08	masses		0.73
B ¹⁰	18.4	8.55	0.25	2.1	A	8.33±0.10	masses		6.33
B ¹¹	81.6	11.50	0.25	1.0	A	11.32±0.10	masses		14.44
Na ²³	100	12.05	0.20	2.5	A	11.7±0.5	masses		13.75
Mg ²⁴	77.4	16.55	0.25	1.9	A	16.2±0.3	(γ, n)	2b	15.31
Mg ²⁶	11.5	7.25	0.20	1.4	A	7.1±1.0	masses		7.54
Mg ²⁶	11.1	11.15	0.20	1.1	A	12.0±0.9	masses		12.13
Al ²⁷	100	12.75	0.20	2.0	A	{11.1±2.0 14.0±0.4	masses (γ, n)	2b	13.70
Si ²⁹	6.2	8.45	0.20	1.0	A	8.48±0.01	(<i>d, p</i>)	‡	8.17
Si ³¹	100	12.05	0.20	3.1	A	12.35±0.2	(γ, n)	2b	13.67
S ³⁴	4.2	10.85	0.20	1.3	A	11.0±0.7	masses		12.48
Cl ³⁵	75.4					9.6±1.4	masses		13.67
		9.95	0.20	1.6	C				
Cl ³⁷	24.6					9.5±0.2	masses		11.58
V ⁵¹	100	11.15	0.20	1.4	A				10.70
Cr ⁵²	83.8	11.80	0.25	2.3	B				11.45
Cr ⁵³	9.4	7.75	0.20	1.6	B				7.35
Mn ⁵⁵	100	10.00	0.20	1.4	A	10.15±0.2	(γ, n)	2c	10.92
Fe ⁵⁶	91.6	11.15	0.25	1.4	A	≥11.3	(<i>d, p</i>)	1	11.62
Fe ⁵⁷	2.1	7.75	0.20	1.5	A	{7.65±0.10 7.63	(<i>d, p</i>) (<i>n, \gamma</i>)	1 §	7.76
Co ⁵⁹	100	10.25	0.20	1.5	A				11.13
Cu ⁶³	70.1	10.85	0.20	1.5	A	10.9±0.2	(γ, n)	2b	11.31
Cu ⁶⁵	29.9	9.75	0.20	1.4	A	10.2±0.2	(γ, n)	2a, 2b	10.26
Zn ⁶⁴	50.9	11.65	0.20	1.1	A	11.8±0.2	(γ, n)	2a, 2c	11.93
Zn ⁶⁶	27.3	11.15	0.20	0.7	B				10.85
Zn ⁶⁷	3.9	7.00	0.20	2.0	A				7.48
Zn ⁶⁸	17.4	10.15	0.20	1.4	B				9.86
Ga ⁶⁹	61.2	10.10	0.20	1.8	B				10.46
Ga ⁷¹	38.8	9.05	0.20	1.6	B				9.55
As ⁷⁶	100	10.10	0.20	1.6	A	10.3±0.2	(γ, n)	2f	9.78
Se ^(?)		7.30	0.20	1.6	C				
Se ^(?)		9.35	0.20	2.4	C				
Br ⁷⁹	50.6	10.60	0.20	1.5	A	10.7±0.2	(γ, n)	2a, 2b	10.00
Br ⁸¹	49.4	9.95	0.20	1.4	A	10.2±0.2	(γ, n)	2a, 2b	9.22
Sr ⁸⁶	9.9	9.50	0.20	1.9	B				9.92
Sr ⁸⁷	7.0	8.40	0.20	1.4	A	{8.42 8.52±0.2	(<i>n, \gamma</i>) (<i>d, p</i>)	§ 1	7.18
Sr ⁸⁸	82.6	11.15	0.20	1.6	B				9.19
Cb ⁹³	100	8.70	0.20	1.6	A				9.86
Mo ^(?)		6.75	0.25	2.0	C				
Mo ^(?)		7.95	0.25	2.0	C				
Ru ^(?)		7.05	0.20	1.9	C				
Ru ^(?)		9.50	0.20	1.6	C				
Rh ¹⁰³	100	9.35	0.20	1.6	A				9.58
Pd ^(?)		7.05	0.20	2.1	C				
Pd ^(?)		9.35	0.20	1.6	C				
Ag ¹⁰⁹	48.1	9.05*	0.20	2.5	B	9.3±0.5	(γ, n)	2a	9.20
Cd ¹¹³	12.3	6.55	0.20	2.0	A	6.44±0.15	(γ, n)	2c	6.80
In ¹¹⁵	95.5	9.05*	0.20	1.9	B	9.5±0.5	(γ, n)	see 1	8.85
Sn ¹¹⁸	22.5	9.10	0.20	1.8	B	{9.33 9.37±0.2	(<i>n, \gamma</i>) (<i>d, p</i>)	§ 1	8.68
Sn ¹¹⁹	9.8	6.60	0.20	1.5	B	6.51±0.15	(γ, n)	2c	6.57
Sb ¹²¹	56					9.25±0.2	(γ, n)	2a, 2b	8.54
		8.95	0.25	2.3	C				
Sb ¹²³	44								8.07
Te ^(?)		6.50	0.20	1.9	C				
Te ^(?)		8.55	0.20	1.7	C				
I ¹²⁷	100	9.10	0.20	1.5	A	{9.3±0.2 9.45±0.2	(γ, n) (γ, n)	2b 2f	8.27
Cs ¹³³	100	9.05	0.20	1.7	A				8.03
Ba ^(?)		6.80	0.20	2.0	C				
Ba ^(?)		8.55	0.25	1.7	C				
La ¹³⁹	100	8.80	0.20	1.6	A	≥8.60	Calc.	See text	7.78

* These values could be influenced by the presence of a second unresolved isotope.
 † C. F. v. Weizsäcker, Z. Physik 96, 431 (1935); N. Bohr and J. A. Wheeler, Phys. Rev. 56, 426 (1939); E. Fermi, Nuclear Physics (University of Chicago Press, Chicago, 1950), p. 7.
 ‡ Endt, Van Patter, and Bueckner, Phys. Rev. 81, 317 (1951).
 § Kinsey, Bartholomew, and Walker, Phys. Rev. 78, 77 (1950); 78, 481 (1950); Bartholomew, Kinsey, and Walker, Phys. Rev. 79, 218 (1950).

TABLE I.—Continued.

Isotope	Percent abundance	Present measurements			Class	Previous measurements		Reference	Threshold from mass formulas†
		Threshold (Mev)	Error (Mev)	m		Threshold (Mev)	Method		
Ce ¹⁴⁰	89	9.05	0.20	1.4	B				8.09
Ce ¹⁴²	11	7.15	0.20	1.5	B				7.70
Ta ¹⁸¹	100	7.55	0.20	1.8	A	7.7±0.2	(γ, n)	2b	7.49
W ^(?)		6.25	0.30	1.0	C				
W ^(?)		7.15	0.30	1.6	C				
Re ¹⁸⁷	61.8	7.30*	0.30	1.5	B				7.35
Ir ¹⁹³	61.5	7.80*	0.20	1.7	B				7.23
Pt ¹⁹⁴	30.2	9.50	0.20	1.3	B				7.44
Pt ¹⁹⁵	35.3	6.10	0.20	1.6	A	6.1±0.1	(γ, n)	2g	
						6.14±0.2	(d, p)	1	6.02
Pt ¹⁹⁶	26.6	8.20	0.20	1.6	B	8.0±0.2	(d, p)	1	7.17
Au ¹⁹⁷	100	7.90	0.20	1.7	A	8.00±0.15	(γ, n)	2c	
						8.10±0.10	(γ, n)	2g	7.38
Tl ²⁰³	21.9	8.80	0.20	1.6	A				7.26
Tl ²⁰⁵	70.9	7.55	0.20	1.1	A	7.48±0.15	(γ, n)	2c	
						7.7±0.2	(d, t)	5	7.02
Pb ²⁰⁷	22.6	6.75	0.20	1.3	A	6.737±0.01	(n, γ)	§	5.85
Pb ²⁰⁸	52.3	7.30	0.20	1.0	A	7.38±0.01	(n, γ)	§	6.96
Bi ²⁰⁹	100	7.40	0.20	1.7	A	7.44±0.05	(d, t)	5	7.16

disintegration energy of Ba¹³⁹ is, however, higher than the present accepted value.⁷ We computed from the above cycle a lower limit of 8.6 Mev for the threshold of La¹³⁹, which is then in agreement with our (γ, n) threshold of 8.8 Mev.

Lanthanum is a nucleus with 82 neutrons. The value of 8.8 Mev reduces the magnitude of the discontinuity in neutron binding occurring at this closed shell. However, the data for Cs¹³³, Ce¹⁴⁰, and Ce¹⁴² in Table I provide additional evidence for a closed shell in this region.

The values of the exponent m in the relation

⁷ Nuclear Data, National Bureau of Standards Circular 499, September 1950.

$Y \sim (E - E_0)^m$ have been included in Table I to completely define the data for each of the isotopes. The yield may also be expressed by the relation

$$Y = \int_{E_0}^{E_{\max}} \sigma(E) P(E, E_{\max}) \eta(E) dE,$$

where $\sigma(E)$ is the cross section for the reaction at the energy E , $P(E, E_{\max})$ represents the bremsstrahlung distribution, and $\eta(E)$ is the detection efficiency of the apparatus. It should be possible, then, from measurements of m and E_0 , to obtain experimental information regarding the behavior of σ in the vicinity of threshold, provided P and η are sufficiently well known. Our present information does not permit such computations.